Solid State Communications 251 (2017) 35–38

Contents lists available at ScienceDirect

Solid State Communications

journal homepage: www.elsevier.com/locate/ssc

Communication

Temperature-dependent photovoltage response in $La_{0.9}Li_{0.1}MnO_3/SrTiO_3$-Nb heterojunction induced by a low intensity pulse laser

Jianyuan Wang*, Jianying Bai, Hui Xing, Shuanhu Wang, Min Wang, Kexin Jin, Changle Chen

Ministry of Education (MOE), Key Laboratory of Space Applied Physics and Chemistry of the Ministry of Education, Northwestern Polytechnical University, Xi'an 710072, China

ARTICLE INFO

Keywords:
A. Manganite
C. Heterojunction
D. Photovoltage

ABSTRACT

The photovoltage response under low intensity pulse laser (473 nm) in the perovskite manganite *p-n* junction $La_{0.9}Li_{0.1}MnO_3/SrTiO_3$:Nb is investigated within a wide temperature range. The maximum photovoltage occurs at around the metal-insulator transition temperature ($T_{MI,}$ ~250 K) of $La_{0.9}Li_{0.1}MnO_3$ rather than the lowest temperature, which indicates that the low density charge induced by a weak light can be significantly affected by the leakage rather than the thermal carriers. Moreover, the time response of photovoltage shows distinct temperature-dependent and light intensity-dependent regularities in the temperature regions $T < T_{MI}$ and $T > T_{MI}$ respectively. The mechanisms are discussed according to the charge transport and magnetic phase transition of $La_{0.9}Li_{0.1}MnO_3$.

1. Introduction

Since the discovery of the colossal magnetoresistance effect in La-Ba-Mn-O and La-Ca-Mn-O [1,2], the properties and mechanisms in a series of doped- manganites ($R_{1-x}A_xMnO_3$, R=La, Pr, A=Ca, Sr, Ba et al.) have been investigated extensively [3–6]. As A is +1 or +2 valence ions, manganites exhibit *p*-type semi-conductivity. Thus, *p-n* junctions can be fabricated with some electronic conductive materials such as *n*-type Si [7], ZnO [8] and Nb-doped $SrTiO_3$(STON) [9], among which the doped-manganite/STON junction is the most probably to get high quality epitaxial growth and stable heterostructure because STON and manganite show similar lattice parameters in *a* and *b* axes. Doped-manganite/STON heterojunction, such as $La_{0.7}Sr_{0.3}MnO_{3-\delta}$/STON [10], $L_{0.67}Ca_{0.33}MnO_{3-\delta}$/STON [11] and $La_{0.9}Ba_{0.1}MnO_3$/STON [12] is a combination of wide band gap semiconductor (STON ~3.2 eV) and a relative narrow one (Manganite ~1.0–1.3 eV) [13,14]. Photo-electric properties with visible light [13] and ultraviolet [14] have been discovered, and the dependence on the irradiation wavelength is discussed [15,16]. Different from the traditional *p-n* junction, the transportation and magnetism mechanisms of doped-manganite are complicated, such as the classic double-exchange theory [17], electron-photo coupling [18], phase separation [19] and percolation theory [20], which result in attractive external field-induced effects on the rectifying and photoelectric properties [21,22]. However, further systematic investigations are needed to find the regularity and internal mechanism on the photo-electric behaviours in the manganite/STON junctions.

In our previous publication [23], photovoltage response to 248 nm pulse laser in $La_{0.9}Li_{0.1}MnO_3$/STON *p-n* junction has been investigated. In this work, in order to explore the wavelength dependent mechanism of the generation and migration of the photo-induced carriers, 473 nm pulse laser is used to excite the photovoltage of $La_{0.9}Li_{0.1}MnO_3$/STON *p-n* junction. Different time response characteristics under this visible laser is discussed and compared with those induced by the ultraviolet. It is also needs to be pointed out that the study on photovoltage with visible light is more possible for practical applications.

2. Experimental

The $La_{0.9}Li_{0.1}MnO_3$(LIMO) target is sintered form the single phase powder which is synthesized by Sol-Gel method. The LIMO film is deposited on 0.5 wt% Nb -doped SrTiO3 (100) substrate by pulse laser deposition. The parameters in these steps can be seen in Ref [23]. The XRD pattern in Fig. 1 indicates a good epitaxial growth of the LIMO film with the substrate STON (100). The thickness of the film measured by SpecEI-2000-VIS ellipsometer is about 110 nm. The wires are connected to the LIMO and STON layers by indium electrodes which are prove to be ohmic contact. To get the temperature-variable condition, the sample is located in Janis CCS-300 refrigerator cryostat system. *I-U* properties are measured by KEITHLEY 2400. The photovoltage is induced by 473 nm pulse laser controlled by a square wave chopper. The frequency is adjusted to make sure that the photovoltage

* Correspondence to: Postal address: Northwestern Polytechnical University, P.O. Box 887, Chang'an district, Xi'an 710072, China.
E-mail address: wangjy@nwpu.edu.cn (J. Wang).

http://dx.doi.org/10.1016/j.ssc.2016.12.012
Received 8 August 2016; Received in revised form 25 October 2016; Accepted 18 December 2016
Available online 20 December 2016

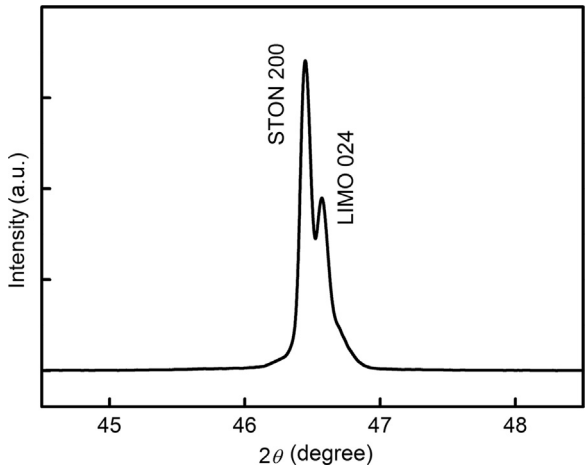

Fig. 1. X-ray diffraction pattern of the LIMO/STON heterojunction.

reaches balance state and recovers to zero during the irradiating and dark period respectively. The voltage signal is captured by Tektronix 500 MHz oscilloscope.

3. Results and discussion

3.1. Current-voltage properties of the p-n junction

Rectifying properties have been found in LIMO/STON heterojunction [23], while an enlarged detail supplies more information in low voltage region. Fig. 2(a) shows the *I-U* curves in 0–0.1 V. It is clear that the current *I* decreases monotonically with the increase of temperature in the range from 40 to 260 K. However, it locates between the values of 200 and 260 K if the temperature rises up to 300 K. Also, the maximum junction resistance (R_j) appears at 260 K, as shown in the inset of Fig. 2(a). Similar performance at the negative voltage region is plotted in Fig. 2(b). The minimum reverse leakage current (I_k) drops with increasing *T*, but rises when $T > 260$ K, as shown in the inset of Fig. 2(b). Both the maximum R_j and the minimum I_k occur at 260 K, which is near T_{MI} (~250 K) for the LIMO layer. It can be concluded that metal-insulator transition in LIMO layer plays an important role in the temperature-dependent changing of *I-U* properties.

3.2. Temperature-dependent photovoltage

When 473 nm pulse laser illuminates on this LIMO/STON junction, photo-induced electrons and holes in LIMO layer are generated. When these electrons and holes arrive at the junction region by diffusion, the "built-in" electric field (*n*-layer→*p*-layer) sweeps electrons towards *n*-STON layer and stops the holes from getting across. Therefore, positive and negative charges are separated, and photovoltage is produced.

The voltage signals (U_{OC}) on this *p-n* junction induced by the irradiation of 473 nm pulse laser is recorded in the temperature range from 20 to 300 K. The resistance of the oscilloscope is set as 1 MΩ to make sure that U_{OC} is measured in an approximate open circuit state [23]. Under a light intensity of 2.5 mW/mm^2, the responses of U_{OC} in one period at different temperatures are presented in Fig. 3(a). U_{OC} increases gradually to a balance value (U_p) at the irradiating period (t=0–0.05 s), and decreases to zero during the dark period (t=0.05–0.1 s). It is obvious that U_p is affected by *T*, and the relationship between U_p and *T* is shown in the inset of Fig. 3(a). The maximum U_p occurs at 240 K, which is also close to the T_{MI} of LIMO layer. Generally, low temperature may lead to the large photovoltage for a *p-n* junction since the concentration of thermal charge carriers is reduced at low temperature. However, U_p is far below the diffusion voltage (0.5–0.8 V [23]) with a weak illumination, which suggests that the density of photo-induced carriers is also far away from the saturated value and the effect of leakage on the carriers should not be ignored. At low temperature region, significant effect from the leakage has been produced, whereas the maximum U_p occurs at around the minimum I_k with temperature around T_{MI}.

Numerical analysis indicates that the U_{OC}-*T* curves in irradiating and dark period are both fitted by exponential functions. For the rising process, it can be expressed in *Eq.*(1):

$$U_{OC} = U_P \cdot [1 - \exp(-t/\tau_1)] \quad (1)$$

Here, *t* and τ_1 represent time and the time constant, respectively. As show in Fig. 3(b), τ_1 varies from 1.61 to 5.11 ms, which is much longer than that (27.7–93.0 μs) under a high-intensity ultraviolet [23]. The time constant during rising process is mainly related to the generation and migration of the photo-induced carrier. In our previous work, 248 nm laser can excite photo-induced carriers in both LIMO layer and STON layer. The "built-in" electric field sweeps the electrons from *p*-LIMO towards *n*-STON layer, and the holes were swept from *n*-STON to the *p*-LIMO layer. High concentration photo-induced carriers and bidirectional migration between *p* and *n* layers result in a short time constant for the rising process. By contrast, the photovoltage excited by 473 nm laser results from the photo-induced carriers only in the LIMO layer, and which is a unidirectional migration from LIMO layer to STON layer. With the rise of *T*, τ_1 decreases after reaching the maximum at T_{MI}, 250 K. The change is caused by the temperature-dependent transition from metallic state to insulator state. Below T_{MI}, double exchange effect among Mn^{3+}-O^{2-}-Mn^{4+} supplies main contribution for the transportation [13] and the migration of carriers is effected by the parallelism degree of the e_g electronics spin. When the

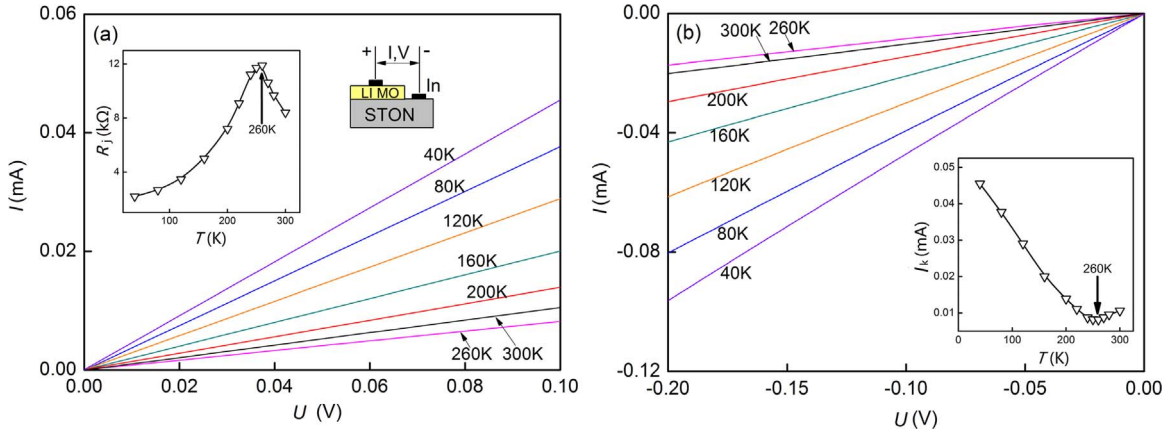

Fig. 2. *I-U* characteristics of LIMO/STON heterojunction at different temperatures: (a) At positive voltage (0–0.1 V). The inset is the relationship between junction resistance R_j and temperature *T*; (b) At negative voltage (−0.2–0 V). The inset is the leakage current when U=−0.1 V.

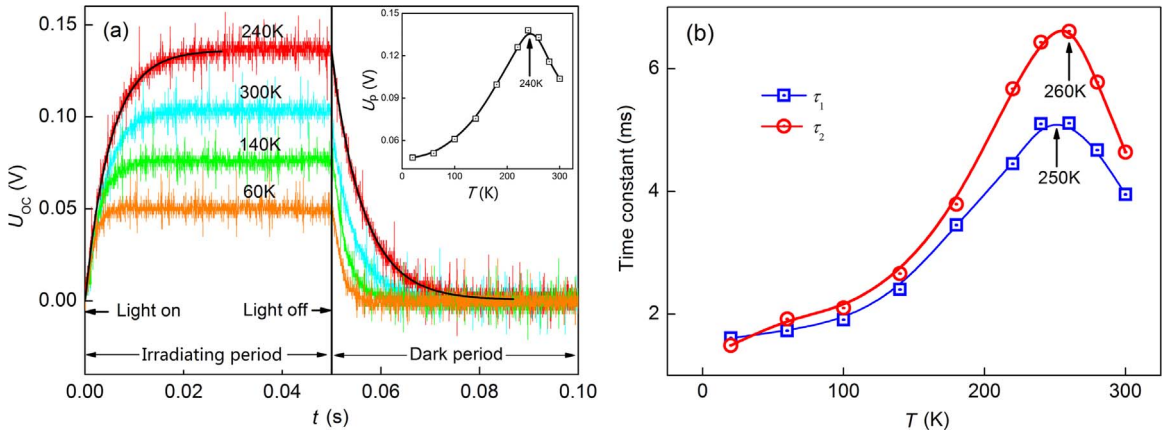

Fig. 3. Photovoltage in LIMO/STON heterojunction under 2.5 mW/mm^2 pulse laser: (a) Time response of U_{OC} within one period. The black curves are exponential fittings for the rising and decaying process. The inset is the balance photovoltage U_p during the irradiating period as a function of temperature; (b) Time constant during the rising process (τ_1) and decaying process (τ_2) at different temperatures.

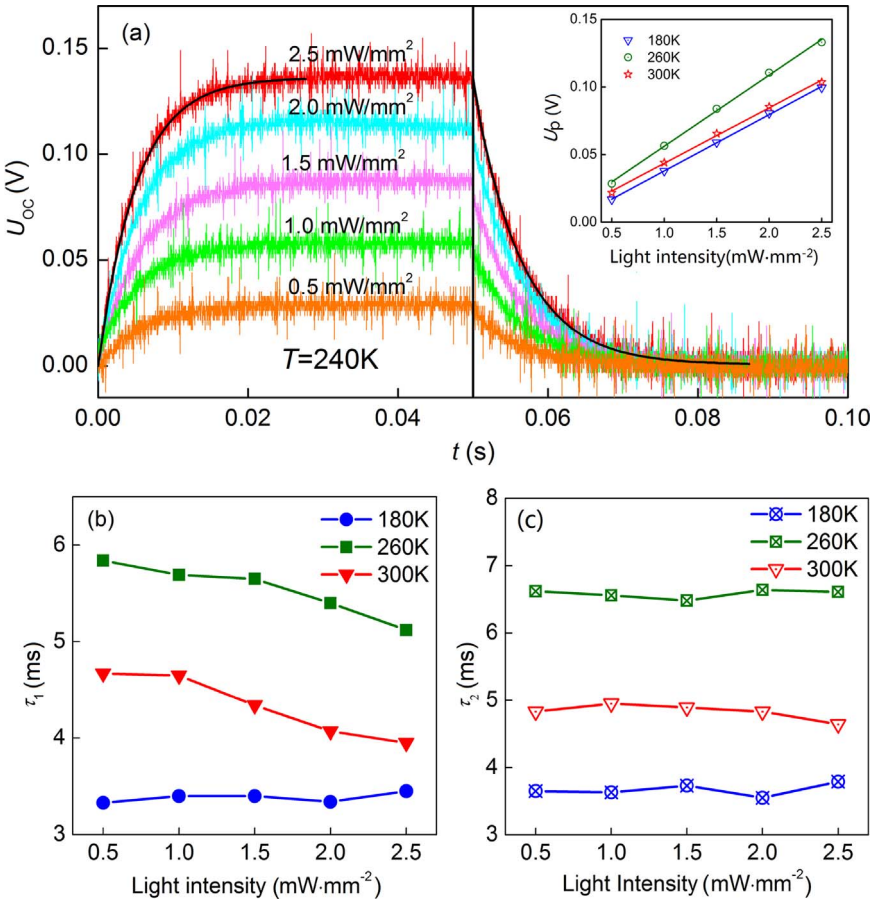

Fig. 4. Photovoltage in LIMO/STON heterojunction with different light intensity: (a) Time response of U_{OC} within one period at 240 K; Time constants τ_1 (b) and τ_2 (c) *versus* light intensity. The inset is U_p*versus* light intensity at 180, 260, and 300 K, and the solid lines are the linear fittings.

temperature increases, the ferromagnetism becomes weak and the parallelism degree gets low. In this case, it takes more time for the carriers' migration to the depletion layer. Above T_{MI}, LIMO exhibits insulator state, small-polaron transportation plays the dominant role for the charge transportation. The delocalization of the carriers is enhanced and long range interaction probably happens between small-polarons as the temperature increases.

During the dark period, there exists the relationship:

$$U_{OC} = U_P \cdot \exp[-(t - t_0)/\tau_2] \quad (2)$$

Here, τ_2 is time constant and t_0 is the duration of irradiating period (0.05 s). Since the approximate open-circuit state has been proved, τ_2 corresponds to the lifetime of nonequilibrium carriers. It can be seen that τ_2 varies between 1.49 and 6.61 ms in Fig. 3(b). The value of τ_2 is close to that (1.80–7.10 ms) under a high-intensity ultraviolet [23]. The similar values could result from the irrelevance between nonequilibrium carriers' annihilation process and the specialty of the light illumination.

3.3. The effect of light intensity on the photovoltage

Photovoltage responses to different light intensities from 0.5 to 2.5 mW/mm^2 in the temperature range of 20–300 K are measured, and the typical performance at T=240 K is plotted in Fig. 4(a). It is found that U_p linearly increases with increasing light intensity at different temperatures, as shown in the inset of Fig. 4(a), which further proves that the light intensity is far below the saturation intensity. As seen in Fig. 4(b), τ_1 is nearly invariable at 180 K but decreases at 260 and 300 K with light intensity increases. The different changing tendency of τ_1 constant below and above T_{MI} is due to the different mechanisms for the interaction between light and LIMO. For the insulator state ($T > T_{MI}$), the excitation from a strong laser can enhance the long range interaction among local polarons. At the same time, higher laser intensity can produce deeper penetration, which shortens the charge transportation distance. Both above mechanisms reduce the time constant τ_1. For the metallic state ($T < T_{MI}$), the increasing illumination intensity brings stronger demagnetization, weakens the spinning parallelism and the double-exchange effect. This results in the enhancement of τ_1, which is an opposite effect to the deeper penetration. The competition between the two mechanisms leads to a relatively stable value of τ_1. Fig. 4(c) illustrates that τ_2 is invariable with different light intensities at 180, 260 and 300 K, indicating that the annihilation of photo-induced carriers is localized.

4. Conclusions

The temperature-dependent photovoltage response under a weak 473 nm pulse laser in the perovskite p-n junction LIMO/STON is investigated. The I-U property in the low bias voltage region shows that both R_j and I_k reach their maximums at 260 K, which is near around T_{MI} of LIMO. The photovoltage U_{OC} exhibits exponential rising to the balance value U_p and then decays to zero with the excitation of 2.5 mW/mm^2 pulse laser. Within a wide temperature range from 20 to 300 K, U_p reaches the peak value at 240 K, which is nearly consistent with the minimum leakage temperature. This indicates that low density charge generated by a weak laser can be significantly affected by the leakage rather than temperature. Moreover, the relationships between τ_1 andτ_2 constants and temperature differ in $T < T_{MI}$ and $T > T_{MI}$ regions. τ_1 decreases with increasing light intensity when $T > T_{MI}$ but keeps invariable if $T < T_{MI}$. Above temperature-dependent I-U property and photovoltage are related to the transition of metal to insulator as well as ferromagnetism to non-ferromagnetism.

Acknowledgements

This work was supported by the National Natural Science Foundation of China (Grant numbers 51402240, 51471134, 61471301 and 51572222); Fundamental Research Fund for the Central Universities of China (Grant number 3102014KYJD026), and the “NWPU Ao Xiang Xin Xing” Foundation (Grant number 2015) in NWPU.

References

[1] R. von Helmolt, J. Wecker, B. Holzapfel, L. Schultz, K. Samwer, Phys. Rev. Lett. 71 (1993) 2331–2333.
[2] S. Jin, T.H. Tiefel, M. McCormack, R.A. Fastnacht, R. Ramesh, L.H. Chen, Science 264 (1994) 413–415.
[3] X.H. Zhang, Z.Q. Li, W. Song, X.W. Du, P. Wu, H.L. Bai, E.Y. Jiang, Solid State Commun. 135 (2005) 356–360.
[4] S. Schramm, J. Hoffmann, Ch Jooss, J. Phys: Cond. Mater. 20 (2008) 395231.
[5] G.T. Tan, S. Dai, P. Duan, Y.L. Zhou, H.B. Lu, Z.H. Chen, Phys. Rev. B 68 (2003) 014426.
[6] A. Urushibara, Y. Moritomo, T. Arima, A. Asamitsu, G. Kido, Y. Tokura, Phys. Rev. B 51 (1995) 14103–14109.
[7] K.X. Jin, S.G. Zhao, X.Y. Tan, C.L. Chen, J. Phys. D: Appl. Phys. 41 (2008) 045105.
[8] K.X. Jin, S.G. Zhao, C.L. Chen, J.Y. Wang, B.C. Luo, Appl. Phys. Lett. 92 (2008) 112512.
[9] J.R. Sun, B.G. Shen, Z.G. Sheng, Y.P. Sun, Appl. Phys. Lett. 85 (2004) 3375–3377.
[10] N. Nakagawa, M. Asai, Y. Mukunoki, T. Susaki, H.Y. Wang, Appl. Phys. Lett. 86 (2005) 082504.
[11] F.X. Hu, J. Gao, J.R. Sun, B.G. Shen, Appl. Phys. Lett. 83 (2003) 1869–1871.
[12] H. Tanaka, J. Zhang, T. Kawai, Phys. Rev. Lett. 88 (2002) 027204.
[13] T. Muramatsu, Y. Muraoka, Z. Hiroi, Solid State Commun. 132 (2004) 351–354.
[14] J.R. Sun, C.M. Xiong, B.G. Shen, P.Y. Wang, Y.X. Weng, Appl. Phys. Lett. 84 (2004) 2611–2613.
[15] J. Dho, Solid State Commun. 150 (2010) 2243–2247.
[16] J.R. Sun, C.H. Lai, H.K. Wong, Appl. Phys. Lett. 85 (2004) 37–39.
[17] C. Zener, Phys. Rev. 82 (1951) 403–405.
[18] A.J. Millis, B.I. Shraiman, R. Mueller, Phys. Rev. Lett. 77 (1996) 175.
[19] Ch Renner, G. Aeppli, B.G. Kim, Y.A. Soh, S.W. Cheong, Nature 416 (2002) 518–521.
[20] J. Blasco, J. García, J.M. de Teresa, M.R. Ibarra, P.A. Algarabel, C. Marquina, J. Phys.: Cond. Mater. 8 (1996) 7427–7430.
[21] J.R. Sun, C.M. Xiong, B.G. Shen, P.Y. Wang, Y.X. Weng, Appl. Phys. Lett. 84 (2004) 2611–2613.
[22] C. Luo, K.X. Jin, C.L. Chen, T. Wu, Appl. Phys. Lett. 103 (2013) 212401.
[23] J.Y. Wang, W. Zhai, B.C. Luo, K.X. Jin, C.L. Chen, Solid State Commun. 187 (2014) 10–12.